Brazilian Journal of Physics
ISSN: 0103-9733
luizno.bjp@gmail.com
Sociedade Brasileira de Física
Brasil

Teixeira, A. M. R.; Santos, H. S.; Albuquerque, M. R. J. R.; Bandeira, P. N.; Rodrigues, A. S.; Silva, C. B.; Gusmão, G. O. M.; Freire, P. T. C.; Bento, R. R. F.
Vibrational Spectroscopy of Xanthoxyline Crystals and DFT Calculations
Brazilian Journal of Physics, vol. 42, núm. 3-4, julio-diciembre, 2012, pp. 180-185
Sociedade Brasileira de Física
São Paulo, Brasil

Braz J Phys (2012) 42:180–185
DOI 10.1007/s13538-012-0075-0

CONDENSED MATTER

Vibrational Spectroscopy of Xanthoxyline Crystals and DFT Calculations

A. M. R. Teixeira · H. S. Santos · M. R. J. R. Albuquerque · P. N. Bandeira · A. S. Rodrigues · C. B. Silva · G. O. M. Gusmão · P. T. C. Freire · R. R. F. Bento

Received: 3 August 2011 / Published online: 31 March 2012

Abstract The Fourier transform infrared and Fourier transform Raman spectra of xanthoxyline crystals are reported, along with ab initio computations of the vibrational spectrum of the xanthoxyline molecule. The infrared and Raman spectra were recorded at 300 K in the 400- to 4,000- and 40- to 4,000-cm^{-1} intervals, respectively. The vibrational wave numbers and wave vectors were obtained from a density functional computation with the 6-31 G(d,p) basis set and the B3LYP approximation to the exchange correlation functional. Comparison with the theoretical results allows assignment of normal modes to the prominent features of the recorded spectra.

Keywords Raman scattering · Infrared scattering · Normal modes · Xanthoxyline crystal

A. M. R. Teixeira
Departamento de Física, Universidade Regional do Cariri,
Juazeiro do Norte, Ceará 63010-970, Brazil

H. S. Santos · M. R. J. R. Albuquerque · P. N. Bandeira · A. S. Rodrigues
Coordenação de Quımica, Universidade Estadual Vale do Acaraú,
Sobral, Ceará 62040-370, Brazil

C. B. Silva · G. O. M. Gusmão · P. T. C. Freire
Departamento de Física, Universidade Federal do Ceará,
Fortaleza, Ceará 60455-760, Brazil

R. R. F. Bento (✉)
Instituto de Física, Universidade Federal do Mato Grosso,
Cuiabá, Mato Grosso 78060-900, Brazil
e-mail: ricardobento@fisica.ufmt.br

1 Introduction

The genus *Croton* of the plant family Euphorbiaceae is widespread in northeastern Brazil. Its application in popular medicine to treat a variety of diseases—cancer, constipation, diabetes, digestive problems, dysentery, external wounds, fever, hypercholesterolemia, hypertension, inflammation, intestinal worms, malaria, pain, ulcers, and weight loss—has been reported by Carneiro et al. [1]. Phytochemical investigations have shown that plants in this genus produce alkaloids [2, 3], flavonoids [4–6], triterpenoids, and steroids [7, 8], and a large number of diterpenoids [9–13].

Croton nepetaefolius in particular, an aromatic plant native to the region, has been extensively used as a sedative, Orexigen, and antispasmodic agent [14]. The chromatographic analysis of the ethanolic extract of *C. nepetaefolius* bark has led to the isolation and characterization of xanthoxyline ($C_{10}H_{12}O_4$), an acetophenone named 2-hydroxy-4,6-dimethoxyacetophenone [15].

Xanthoxyline derivatives, the results of structural modifications, have been studied in search of new drugs. The xanthoxyline derivative 2-(4-bromobenzoyl)-3-methyl-4,6-dimethoxy benzofuran showed potent antispasmodic activity [16]. The benzoyl, acetyl, and tosyl groups were introduced in the hydroxyl group of xanthoxyline, but yielded inactive compounds. By contrast, the benzyl and ρ-methoxybenzyl groups yielded compounds four- to eightfold more potent than xanthoxyline [17]. While highlighting the derivatives, which are perhaps more important than the molecule itself, these studies call for additional research of xanthoxyline. Additional motivation is provided by the remarkable biological and pharmacological properties of acetophenone, a bactericide [18], a fungicide [19], and an antispasmodic [20].

Having found no pertinent vibrational spectroscopical study in the literature, we here report an infrared analysis and a Raman scattering study, in the 40- to 4,000-cm^{-1} spectral range, of a xanthoxyline crystal obtained from the stems of *C. nepetaefolius*. We compare the results of a density functional calculation with the measured spectra and assign normal modes of vibration to the peaks in the spectra.

2 Experimental

The bark of *C. nepetaefolius* was collected in May 2004, in Caucaia, Ceará State, Brazil. The plant material was identified by Edson Paula Nunes at the Ceará Federal University Herbarium, Fortaleza, Brazil, where a voucher specimen (No. 33582) was deposited.

The bark (5.0 kg) of *C. nepetaefolius* was powdered and extracted with ethanol (10 L×3, at room temperature). The solvent was removed under reduced pressure to give an EtOH extract. The EtOH extract (58.2 g) was coarsely fractionated on a silica gel column by elution with *n*-hexane (F 1-15), *n*-hexane/EtOAc 1:1 (F s 16-25), EtOAc (F 26-40), and EtOH (F 41-48), affording a total of 48 fractions of 100 mL each. The fractions *n*-hexane/EtOAc 1:1 (F 16-25; 10.8 g) were pooled and fractionated on a silica gel column using *n*-hexane (F′ 1), *n*-hexane/EtOAc (9:1 F′ 2-10; 7:3 F′ 11-13; 1:1 F′ 14-15) and EtOAc (F′ 16), providing 16 fractions of 100 mL each. The fractions (F′ 10-13) and (F′ 16) obtained with *n*-hexane/EtOAc (7:3) and EtOAc yielded white crystals [mp 77–78.5 °C, MS (70 eV, in percent) *m*/z 196 [M]$^+$, 181 (100), 166 (15), 151 (8), 138 (23), 95 (8)] whose ^{1}H and ^{13}C NMR spectra and other properties coincided with the published values for 2-hydroxy-4,6-dimethoxyacetophenone, listed in Table 1 [15, 21].

The melting point was recorded with a Mettler Toledo, and the ^{1}H and ^{13}C NMR spectra were recorded on a Bruker Avance DRX-500 (500 MHz for ^{1}H and 125 MHz for ^{13}C); chemical shifts were given in parts per million (™$_C$ and ™$_H$), relative to residual $CHCl_3$ (7.24 and 77.0 ppm). Mass spectra were registered by a Shimadzu QP5050A mass spectrometer. Silica gel 60 (230–400 mesh, Merck) was used for analytical TLC. Silica gel 60 (70–230 mesh, Merck) was used for column chromatography. The compound was visualized by TLC using vanillin–perchloric acid–EtOH followed by heating.

The Fourier transform (FT)-Raman spectrum was measured in a Bruker RFS100/S FTR system and D418-T detector, with the sample excited by the 1,064-nm line of an Nd:YAG laser. The infrared spectrum was obtained with an Equinox/55 (Bruker) Fourier transform infrared (FTIR) spectrometer. FT-Raman and FTIR spectra were collected from samples confined in screw cap standard chromatographic glass vials, at the nominal resolution of 4 cm^{-1}, accumulating 60 scans per spectra under 150 mW laser power. To record the IR spectra, we ground the sample in an agate mortar to minimize surface scattering and mixed it with KBr until a uniform pellet resulted. Two Raman spectra were obtained from a slightly compacted powder of the sample in a specific sample holder.

Table 1 Reference data for 2-hydroxy-4,6-dimethoxyacetophenone (from refs. [15, 21])

C	δ_H	δ_C
1		106.22
2		163.12
3	6.04	93.72
4		167.78
5	5.91	90.91
6		166.30
7		203.32
8	2.60	33.04
OH	14.01	
MeO	3.84	55.70
MeO	3.81	55.70

3 Computational Method

Density functional theory (DFT) calculations were carried out with the Gaussian 98 package [22]. The B3LYP functional was used with the 6-31 G(d,p) basis set. The calculation determined the electronic structure of an isolated molecule of xanthoxyline. The optimized structure yielded the vibrational wave numbers, the output file containing the optimized structure, the vibrational frequencies in the harmonic approximation, and the atomic displacements for each mode.

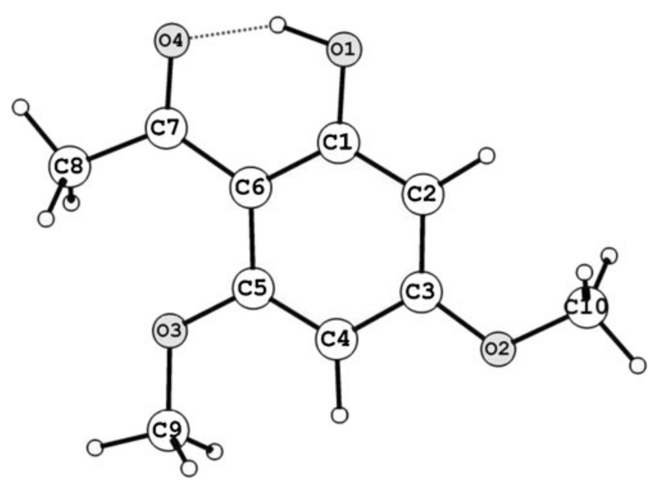

Fig. 1 Molecular structure of xanthoxyline: $C_{10}H_{12}O_4$

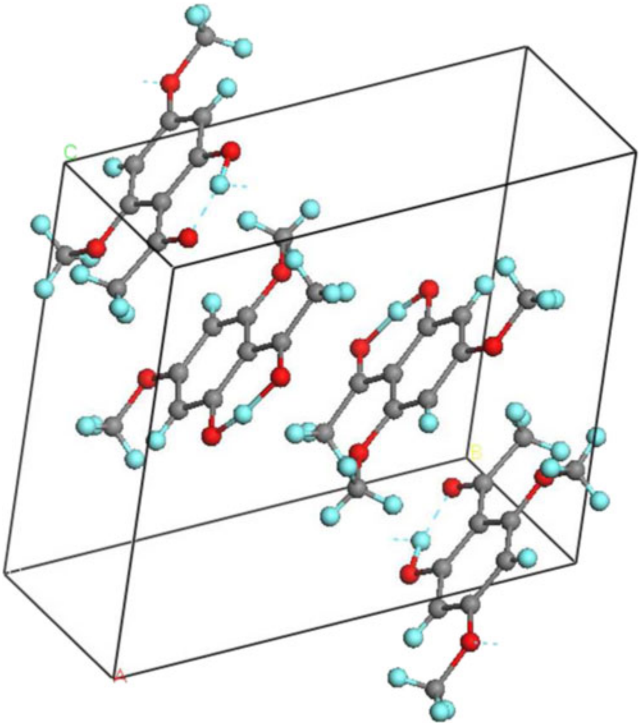

Fig. 2 Representation of the molecules in the crystal structure of xanthoxyline at room temperature

For the optimized structure of the molecule, no imaginary frequency was obtained, showing that the true minimum of the potential energy surface had been found. In Section 4 we compare the calculated vibrational wave numbers with the experimental Raman and IR frequencies.

Several codes for ab initio molecular computation of energies, molecular structures, and vibrational frequencies are available, such as the HyperChem, Spartan, Gamess and Materials Studio, and Quantum Expresso, the last two capable of carrying out DFT calculations of vibrational frequencies of the crystal under study. Our investigation relied on the Gaussian code, which does not calculate crystalline vibrational frequencies. For this reason, our DFT calculations focused on a single molecule in the unit cell of the crystal. Our calculation is thus restricted to the optical modes of the crystal, i.e., blind to the low-wave number lattice vibrations.

4 Results and Discussion

Figure 1 shows the molecular structure of xanthoxyline. The labeling describes the parameters for the optimized structure and molecular wave vectors. At room temperature, the xanthoxyline crystal has triclinic structure with space group P$\bar{1}$, with Z=4 and lattice parameters a=8.0551 Å, b=11.5505 Å, c=11.7068 Å, α=70.590°, β=77.218°, and γ=75.733° [19]. Figure 2 shows the distribution of the four molecules of xanthoxyline in the unit cell at 300 K. The FT-Raman and FT-IR spectra appear in Fig. 3a, b, respectively. The vertical arrow in Figs 3a, b corresponds to the Raman band $\omega_{\text{FT-Raman}}$=965 cm^{-1} and the infrared band $\omega_{\text{FT-IR}}$=965 cm^{-1}, respectively, associated with the atomic displacements in Fig. 4a.

The molecular structure of xanthoxyline in the DFT calculations corresponds to a single molecule of the unit cell described in [19]. This structure is compatible with the NMR data in [15].

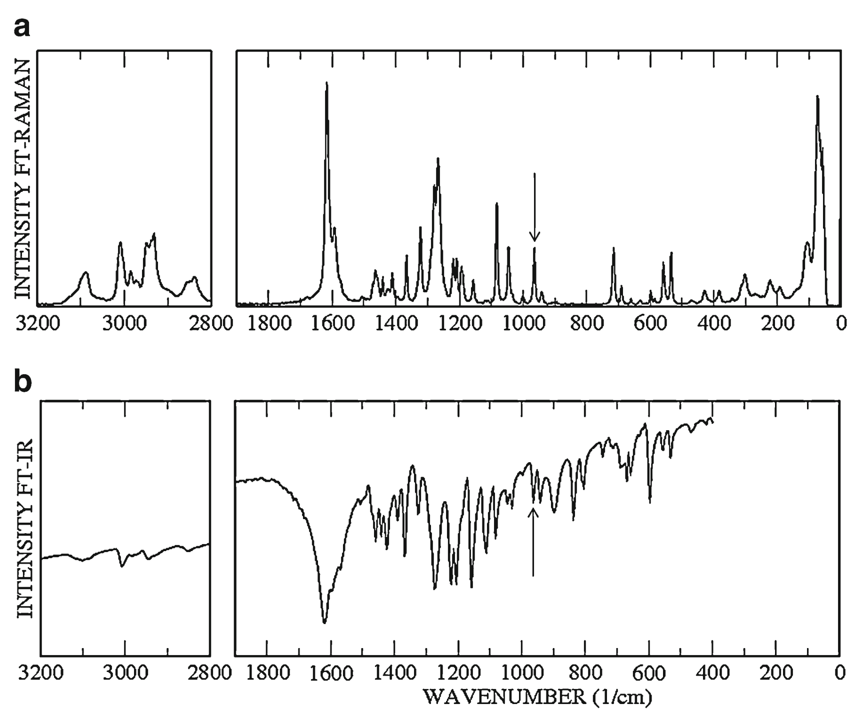

Fig. 3 The spectra of xanthoxyline crystal at room temperature: **a** FT-Raman and **b** FT-IR. The *vertical arrows* in **a** and **b** correspond respectively to Raman band $\omega_{\text{FT-Raman}}$=965 cm^{-1} and the infrared band $\omega_{\text{FT-IR}}$=965 cm^{-1} associated with the atomic displacements in Fig. 4a

The xanthoxyline molecule has 26 atoms and hence 72 modes of vibration. Table 2 lists in details the assignments for the molecular vibrations of the xanthoxyline crystal. The first, second, and third column presents the calculated wave numbers ω_{calc}, the experimental FT-Raman wavenumbers $\omega_{FT\text{-}Ramam}$, and the experimental FT-IR wave numbers $\omega_{FT\text{-}IR}$, respectively. The last column lists the assignments.

The following symbols label the assignments: r = rocking; τ = twisting; sc = scissoring; wag = wagging; δ = deformation; δ_{ip} = in-plane deformation; δ_{oop} = out-of-plane deformation; and ν = stretching, ν_s = symmetric stretching, and ν_{as} = asymmetric stretching. To more clearly describe the molecular vibrations, we denote R the ring containing the benzene functional group type.

The assignment for the crystal shows that most bands in the FT-Raman and FT-IR spectroscopies correspond to mixtures of vibrational modes. Such mixtures are common in molecules of C_1 site symmetry. The superposition of modes precludes direct identification of the bands. This difficulty notwithstanding, the DFT calculation allowed us to describe the assignments of the vibrational modes in detail.

In the 200- to 1,000-cm^{-1} range, the Raman bands have the lowest intensities, while the strongest ones emerge in the 1,250- to 1,700-cm^{-1} range. Vibrations related to the deformation of the ring are observed in the wide spectral range spanning from 50 to 1,691 cm^{-1}. The out-of-plane deformations (γ_{oop}[R]) lie in the $50\leq\omega_{calc}\leq309$ and $585\leq\omega_{calc}\leq956$-cm^{-1} regions, while the in-plane ring deformations (γ_{ip}[R]) occur frequently in the $349\leq\omega_{calc}\leq562$, $969\leq\omega_{calc}\leq1{,}162$, and $1{,}309\leq\omega_{calc}\leq1{,}691$-cm^{-1} regions.

Torsional ring modes are most commonly found in the $50\leq\omega_{calc}\leq309$-cm^{-1} range of calculated wave numbers. In this region we identified nine Raman bands. For example, the out-of-plane deformation γ_{oop}[R][τ (C2C3C4)], responsible for strong Raman bands, is at 105 cm^{-1} (ω_{calc}=106 cm^{-1}).

Scissoring vibrations appear at ω_{calc}=137, 216, and 1,521 cm^{-1}. Most vibrations of this type are nonetheless found in the $299\leq\omega_{calc}\leq606$-cm^{-1} range. Rocking vibrations generate bands in the $660\leq\omega_{calc}\leq1{,}244$-cm^{-1} range. In the $1{,}259\leq\omega_{calc}\leq1{,}497$-cm^{-1} range, wagging vibrations appear.

The 2,800- to 3,200-cm^{-1} range of the Raman spectrum contains stretching vibrations of the CH and CH_3 functional groups. Since no bands were observed above 3,050 cm^{-1}, and since the stretching vibrations of water molecules resonate at 3,400 cm^{-1}, we conclude that the crystal contains no water.

Figure 4 shows atomic displacements corresponding to selected normal modes from the isolated molecular structure of xanthoxyline. Figure 4a shows the atomic displacements associated to the deformations {γ_{ip}[R][sc(C1C2C3)], r(C8H3), ν(C9O13; C10O2)}, which gives rise to the strong band at 965 cm^{-1} (ω_{calc}=969 cm^{-1}). Figure 4b depicts the atomic displacements due to the mixture of the vibrational modes {wag(C9H3;C10H3), sc(C8H3), δ(O1H)}, which corresponds to the calculated wave number ω_{calc}=1,511 cm^{-1}.

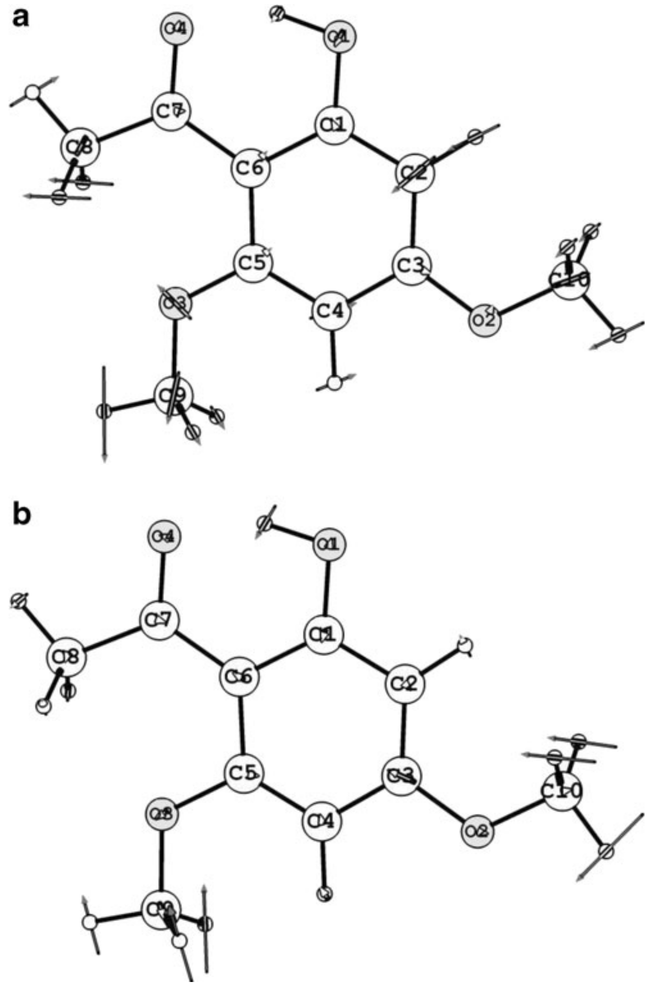

Fig. 4 Selected representations of atomic vibrations corresponding to the calculated wave numbers of molecule xanthoxyline: **a** ω_{calc}=969 cm^{-1} and **b** ω_{calc}=1,511 cm^{-1}

Finally, we comment on the low-frequency bands ($\omega_{calc}\leq$ 200 cm^{-1}), a region of the spectrum that, in our calculation, is punctuated by vibrations of the R ring. We recall, however, that the DFT computation misses the long wavelength vibrations of the lattice and is hence only partially reliable in this range. The first few assignments in Table 2 are therefore only indicative of more complex modes combining the listed vibrations with degenerate acoustic phonon modes (not shown).

5 Conclusions

We have measured the FT-Raman and FT-IR spectra of the xanthoxyline at room temperature and computed the vibrational modes and wave numbers of xanthoxyline molecule with the Gaussian 98 implementation of DFT, the B3LYP exchange correlation functional, and the 6-31 G(d,p) basis

Table 2 Calculed wave numbers, Raman, and IR bands positions in units of per centimeter and assignments for vibrational modes of xanthoxyline

ω_{calc}	$\omega_{FT\text{-}Ramam}$	$\omega_{FT\text{-}IR}$	Assignment
50	59		γ_{oop}[R][τ(O2C10; C7C8)]
84	74		γ_{oop}[R][τ(O3C9; 02C10)]
105	106		γ_{oop}[R][τ(C2C3C4)]
118			γ_{oop}[R][τ(C1C2C3)]
137	145		sc(C3O2C10; C5O3C9)
203	191		γ_{oop}[R][τ(C1C2O1)]
214	222		γ_{oop}[R][τ(C2C3C4)]
216			sc(C3O2C10; C5O3C9; C6C7C8)
228			γ_{oop}[R][τ(C2C3C4)]
254	267		γ_{oop}[R][τ(C5C6C7)]
286			γ_{oop}[R][τ(C2C3C4)]
299	302		γ_{ip}[R][sc(C6C7C8; C3O2C10; C5O3C9)]
309	312	320	γ_{oop}[R][τ(C1C6C7)]
349	341	367	δ_{ip}[R][sc(C6C7C8; C9O3C5)], δ(O1H)
388	383		δ_{ip}[R][sc(C6C7C8; C9O3C5)], δ(O1H)
433	429	420	δ_{ip}[R][sc(C6C7C8; C9O13C5)], δ(O1H)
466	469	467	δ_{ip}[R][sc(C5O3C9; C10O2C3)]
543	535	531	δ_{ip}[R][sc(C1C2C3)]
562	558	556	δ_{ip}[R][sc(C1C5C6)]
585	586	595	γ_{oop}[R][τ(C6C7C8)], δ_{oop}(O4)
606			γ_{ip}[R][sc(C10O2C3)], δ(C7O4)
632	631	630	γ_{oop}[R][τ(C1C5C6)], δ(C2H; C4H)
660	660	657	γ_{oop}[R][τ(C2C3C4)], δ_{oop}[R][δ(C2H; C4H)], r(C8H_3; C9H_3)
703	691	703	γ_{ip}[R][r(C10H_3; C9H_3)]
719	714	713	γ_{ip}[R][ν_s(C1C5C6); sc(C2C3C4)], r(C8H_3; C9H_3)
726		719	γ_{oop}[R][τ(C1C5C6); (C2C3C4)], δ_{oop}(C2H; C4H; O1H)
801			γ_{oop}[R][τ(C3C4C5)], δ_{oop}[R][δ(C4H)]
820	845	836	γ_{oop}[R][wag(C1C2C3)], δ_{oop}[R][δ(C2H)]
956	940	940	γ_{oop}[R][δ(O1H)]
969	965	963	γ_{ip}[R][sc(C1C2C3)], r(C8H_3), ν(C9O13; C10O2)
978			γ_{ip}[R][ν(C1C6)], r(C8H_3), δ(C2H; O1H)
1,031			γ_{ip}[R][sc(C3C4C5)], r(C8H_3), δ(C2H), ν_s(C9O3; C10O2), ν(C1O1)
1,050	1,045	1,045	τ(C8H_3)
1,068	1,083	1,081	γ_{ip}[R][ν_s(C2C3C4); ν(C7C6)], r(C8H_3), δ(C4H; C2H), ν(O2C10)
1,107	1,108	1,111	γ_{ip}[R][ν_s(C2C3C4)], r(C8H_3; C9H_3), δ(C4H; C2H)
1,162	1,157	1,157	γ_{ip}[R][ν(C5C6)], ν(O3C9), r(C8H_3; C10H_3)
1,176			r(C9H_3; C10H_3)
1,177			r(C9H_3;C10H_3)
1,196		1,196	r(C9H_3; C10H_3), δ(C2H; C4H; O1H)
1,216	1,219	1,205	r(C9H_3; C10H_3), δ(C2H; C4H; O1H)
1,244		1,223	r(C9H_3; C10H_3), δ(C2H; C4H), ν(C1O1)
1,259	1,267	1,272	γ_{ip}[R][ν(C1C2)], wag(C9H_3), r(C10H_3), δ(C4H;O1H)
1,309	1,323	1,324	γ_{ip}[R][ν(C1C2; C3C4; C5C6)], wag(C8H_3; C9H_3; C10H_3)
1,352	1,365	1,367	γ_{ip}[R][ν_{as}(C1C2C6); ν(C1O1)], wag(C8H_3; C9H_3; C10H_3), δ(C4H; O1H)
1,371	1,393	1,389	γ_{ip}[R][ν(C5C6); ν_{as}(C2C3C4)], wag(C8H_3; C9H_3; C10H_3), δ(O1H)
1,410	1,411		γ_{ip}[R][ν(C5C6)], wag(C8H_3; C10H_3)
1,455	1,441	1,441	γ_{ip}[R][ν(C2C3; C4C5)], wag(C9H_3; C10H_3), sc(C8H_3), δ(C2H; O1H)
1,464	1,461	1,469	γ_{ip}[R][ν(C2C3; C4C5)], wag(C10H_3), sc(C8H_3; C9H_3), δ(C4H; O1H)
1,473			γ_{ip}[R](ν(C4C5; C1O1)), wag(C9H_3; C10H_3), sc(C8H_3)
1,487			τ(C8H_3)
1,497		1,493	γ_{ip}[R][ν(C1C2O1)], wag(C9H_3; C10H_3), sc(C8H_3), δ(C2H; O1H)
1,504			τ(C9H_3; C10H_3)
1,505	1,506	1,507	τ(C9H_3; C10H_3)
1,511			wag(C9H_3; C10H_3), sc(C8H_3), δ(O1H)
1,518			γ_{ip}[R][ν(C5O3; C3O2)], sc(C8H_3; C9H_3; C10H_3), δ(O1H)
1,521			sc(C9H_3; C10H_3), δ(O1H; C2H)
1,551	1,592	1,597	γ_{ip}[R][ν(C5C6; C3C4)], δ(C4H; O1H), sc(C8H_3; C9H_3; C10H_3)
1,635	1,616	1,619	γ_{ip}[R][ν_{as}(C1C5C6); ν(C2C3)], δ(C2H; O1H)
1,664			γ_{ip}[R][δ(C4H; C2H)], wag(C0H3; C9H3), ν(C7O14)
1,691			γ_{ip}[R][ν(C7O4)], δ_{ip}(C4H)
3,012	3,009	3,005	ν(C11H)
3,028			ν(C11H)
3,029			ν(C9H_3; C10H_3)
3,067			ν(C8H_3)
3,096	3,090	3,089	ν_{as}(C9H_3; C10H_3)
3,097			ν_{as}(C9H_3; C10H_3)
3,139		3,116	ν_{as}(C8H_3)
3,154			ν_{as}(C9H_3)
3,168			ν_{as}(C8H_3)
3,297			ν(C2H)
3,255			ν(C4H)

set. The computation reproduced the spectral features very well. On the basis of this agreement, we have assigned the observed resonant wave numbers to ionic displacements motions in the molecules. Given that stretching vibrations of water molecule are expected at ~3,400 cm^{-1}, the structureless profile in this region indicates that the crystal is devoid of water molecules. Although offering no clues concerning the pharmacological properties of xanthoxyline, our study of its vibrational spectrum yields the quantitative information that future researchers may need to explain the behavior of the material under different thermodynamical conditions.

Acknowledgments The authors would like to acknowledge the financial support from the Brazilian agencies FUNCAP and CNPq. We also thank the CENAPAD-SP for the use of the GAUSSIAN 98 software package and the computational facilities through the project reference proj373.

References

1. V.A. Carneiro, H.S. Santos, F.V.S. Arruda, P.N. Bandeira, M.R.J.R. Albuquerque, M.O. Pereira, H. Mariana, S.C. Benildo, H.T. Edson, Molecules **16**, 190–201 (2011)
2. R.M. Murillo, J. Jakupovic, J. Rivera, V.H. Castro, Rev Biol Trop **49**, 259–264 (2001)
3. V.T. Araujo-Junior, M.S. da Silva, E.V. da Cunha, M.D. Agra, R.N. da Silva, J.M. Barbosa, R. Braz-Filho, Pharm Biol **42**, 62–67 (2004)
4. M.T.L.P. Peres, F.D. Monache, A.B. Cruz, M.G. Pizzolatti, R.A. Yunes, J Ethnopharmacol **56**, 223–226 (1997)
5. M.A.M. Maciel, A.C. Pinto, A.C. Arruda, S.G.S.R. Pamplona, F.A. Vanderlinde, A.J. Lapa, A. Echevarri, N.F. Grynberg, I.M.S. Colus, R.A.F. Faria, A.M.L. Costa, V.S.N. Rao, J Ethnopharmacol **70**, 41–55 (2000)
6. K. Graikou, N. Aligiannis, A.L. Skaltsounis, I. Chinou, S. Michel, F. Tillequin, M. Litaudon, J Nat Prod **67**, 685–688 (2004)
7. M.T.L.P. Peres, F.D. Monache, M.G. Pizzolatti, A.R.S. Santos, A. Beirith, J.B. Calixto, R. Yunes, A Phytother Res **12**, 209–211 (1998)
8. A.B.A. Guadarrama, M.Y. Rios, J Nat Prod **67**, 914–917 (2004)
9. J.D. McChesney, E.R. Silveira, Fitoterapia **61**, 172–175 (1990)
10. S. El Mekkawy, M.R. Meselhy, N. Nakamura, M. Hattori, T. Kawahata, T. Otake, Phytochemistry **53**, 457–464 (2000)
11. P.R. Barbosa, M. Fascio, D. Martins, M.L.S. Guedes, N.F. Roque, Biochem Syst Ecol **31**, 307–308 (2003)
12. P.M. Giang, P.T. Son, J.H. Lee, J.J. Lee, H. Otsuka, Chem Pharm Bull **52**, 879–882 (2004)
13. H.S. Santos, F.W.A. Barros, M.R.J.R. Albuquerque, P.N. Bandeira, C. Pessoa, R. Braz-Filho, F.J.Q. Monte, J.H. Leal-Cardoso, T.L.G. Lemos, J Nat Prod **72**, 1884–1887 (2009)
14. H.S. Santos, F.M.R. Mesquita, T.L.G. Lemos, F.J.Q. Monte, R. Braz-Filho, Quim Nova **31**, 601–604 (2008)
15. A.P.V. Abdon, J.H. Leal-Cardoso, A.N. Coelho-de-Souza, S.M. Morais, C.F. Santos, Braz J Med Biol Res **35**, 1215–1219 (2002)
16. Z.R. Vaz, V.C. Filho, R.A. Yunes, J.B. Calixto, J Pharm Exp Ther **278**, 304–312 (1996)
17. V.C. Filho, O.G. Miguel, R.J. Nunes, J.B. Calixto, R.A. Yunes, J Pharmaceut Sci **84**, 473–475 (1995)
18. G.F. Godoy, O.G. Miguel, E.A. Moreira, Fitoterapia **62**, 269–270 (1991)
19. E.O. Lima, V.M.F. Morais, S.T.A. Gomes, V. Cechinel-Filho, O.G. Miguel, R.A. Yunes. Anais do XIII Simpósio de Plantas Medicinais do Brasil. Fortaleza, Proceedings, (1994) pp. 122
20. A. Suksamrarn, S. Eiamong, P. Piyachaturawat, L.T. Byrnes, Phytochemistry **45**, 103–105 (1997)
21. M.G. Soares, A.P.V. Felippe, E.F. Guimares, M.J. Kato, J. Ellena, A.C. Doriguetto, J Braz Chem Soc **17**, 1205–1210 (2006)
22. M.J. Frisch, G.W. Trucks, H.B. Schlegel, G.E. Scuseria, M.A. Robb, J.R. Cheeseman, V.G. Zakrzewski, J.A. Montgomery, R.E. Stratmann Jr, J.C. Burant, S. Dapprich, J. M. Millam, A.D. Daniels, K.N. Kudin, M.C. Strain, O. Farkas, J. Tomasi, V. Barone, M. Cossi, R. Cammi, B. Mennucci, C. Pomelli, C. Adamo, S. Clifford, J. Ochterski, G.A. Petersson, P.Y. Ayala, Q. Cui, K. Morokuma, P. Salvador, J.J. Dannenberg, D.K. Malick, A.D. Rabuck, K. Raghavachari, J.B. Foresman, J. Cioslowski, J.V. Ortiz, A.G. Baboul, B.B. Stefanov, G. Liu, A. Liashenko, P. Piskorz, I. Komaromi, R. Gomperts, R.L. Martin, D.J. Fox, T. Keith, M.A. Al-Laham, C.Y. Peng, A. Nanayakkara, M. Challacombe, P.M.W. Gill, B. Johnson, W. Chen, M.W. Wong, J.L. Andres, C. Gonzalez, M. Head-Gordon, E.S. Replogle, J.A. Pople. Gaussian 98 (Revision A.11.2). Gaussian: Pittsburgh, PA, (2001)